Bioorganic & Medicinal Chemistry 18 (2010) 7092–7100

Contents lists available at ScienceDirect

Bioorganic & Medicinal Chemistry

journal homepage: www.elsevier.com/locate/bmc

Structure-based virtual screening of novel tubulin inhibitors and their characterization as anti-mitotic agents

Nam Doo Kim [a,d], Eun-Sook Park [b,c], Young Hoon Kim [d], Seung Kee Moon [e], Sung Sook Lee [e], Soon Kil Ahn [f], Dae-Yeul Yu [g], Kyoung Tai No [a,*], Kyun-Hwan Kim [b,c,*]

[a] Department of Biotechnology, College of Life Science and Biotechnology, Yonsei University, Seoul 120-749, Republic of Korea
[b] Department of Pharmacology School of Medicine, and Center for Cancer Research and Diagnostic Medicine, IBST, Konkuk University, Seoul 143-701, Republic of Korea
[c] Research Institute of Medical Sciences, Konkuk University, Seoul 143-701, Republic of Korea
[d] R&D Center, Equispharm Inc., Gyeonggi-do 443-766, Republic of Korea
[e] CKD Research Institute, Chonan Post Office Box 74, Chonan 330-600, Republic of Korea
[f] Department of Biology, College of Natural Science, Incheon University, Incheon 406-772, Republic of Korea
[g] Aging Research Center, Korea Research Institute of Bioscience and Biotechnology 111 Gwahangno, Yuseong-gu Daejeon 305-806, Republic of Korea

ARTICLE INFO

Article history:
Received 4 June 2010
Revised 30 July 2010
Accepted 31 July 2010
Available online 6 August 2010

Keywords:
Microtubule
Colchicine
Virtual screening
Molecular docking
Pharmacophore

ABSTRACT

Microtubule cytoskeletons are involved in many essential functions throughout the life cycle of cells, including transport of materials into cells, cell movement, and proper progression of cell division. Small compounds that can bind at the colchicine site of tubulin have drawn great attention because these agents can suppress or inhibit microtubule dynamics and tubulin polymerization. To find novel tubulin polymerization inhibitors as anti-mitotic agents, we performed a virtual screening study of the colchicine binding site on tubulin. Novel tubulin inhibitors were identified and characterized by their inhibitory activities on tubulin polymerization in vitro. The structural basis for the interaction of novel inhibitors with tubulin was investigated by molecular modeling, and we have proposed binding models for these hit compounds with tubulin. The proposed docking models were very similar to the binding pattern of colchicine or podophyllotoxin with tubulin. These new hit compound derivatives exerted growth inhibitory effects on the HL60 cell lines tested and exhibited strong cell cycle arrest at G2/M phase. Furthermore, these compounds induced apoptosis after cell cycle arrest. In this study, we show that the validated derivatives of compound **11** could serve as potent lead compounds for designing novel anti-cancer agents that target microtubules.

1. Introduction

Microtubules are dynamic cytoskeletal polymers consisting of α/β-tubulin heterodimers that are organized head-to-tail into linear protofilaments[1–3] and are involved in various cellular functions, including intracellular transport of material, movement of cytoplasmic organelles or vesicles, and proper progression of cell division.[4,5] In the mitotic phase of the cell cycle, microtubules are highly dynamic, rapidly assembling, and disassembling according to the cell's needs.[6] Disruptions of the microtubule network can induce cell cycle arrest and ultimately lead to apoptosis. The mitotic spindle, composed of microtubules generated by polymerization of α/β-tubulin heterodimers, has been considered one of the most important targets in treating many types of cancers.[7,8]

Tubulin inhibitors have been known to bind distinct sites within β-tubulin, resulting in the destabilization or stabilization of microtubules and leading to mitotic catastrophe. These agents can be grouped into three classes according to the site of binding on the tubulin molecule.[9] The representative examples are the taxol, vinblastine, and colchicine binding sites. Among these binding sites, the taxol binding site has been most well characterized using the crystal structure of tubulin[5] and the partial overlaps with those of other compounds such as epothilones[10] or eleutherobin.[10] Vinblastine introduces a wedge at the interface of two tubulin molecules and thus interferes with tubulin assembly. Recently, the binding site of vinblastine was reported in the X-ray structure of vinblastine bound to tubulin in a complex with the RB3 protein stathmin-like domain (RB3-SLD).[11] The colchicine binding site was also well characterized in the crystal structure of α/β-tubulin, and was found at the interface of the α-subunit of the α/β heterodimer.[11–13]

Several compounds that target the microtubule have been discovered and developed for cancer treatment.[27] Among these compounds, epothilone, paclitaxel, and vindesine have already been launched in clinical use. Although vinblastine and taxol are effective anti-mitotic agents, they present many problems related to their structural complexities, including difficulty in synthesis and

* Corresponding authors. Tel.: +82 2 2030 7833; fax: +82 2 2049 6192 (K.-H.K.).
E-mail addresses: ktno@yonsei.ac.kr (K.T. No), khkim10@kku.ac.kr (K.-H. Kim).

0968-0896/$ - see front matter © 2010 Elsevier Ltd. All rights reserved.
doi:10.1016/j.bmc.2010.07.072

formulations and poor bioavailability. The rapid emergence of resistance against these drugs has also been reported.[14–17] These problems must be overcome in order to obtain novel anti-mitotic agents with better therapeutic properties.

In this regard, we previously designed novel tubulin inhibitors and evaluated the biological functions.[18] We investigated the structural basis for the interaction of anti-mitotic agents with tubulin and proposed the binding models for compound MDL-27048 in the colchicine binding site on tubulin.[19,20] The proposed model was not only consistent with the results of a previous competition experiment between colchicine and MDL-27048, but also suggested an additional binding cavity on β-tubulin. Based on these findings from the proposed MDL-27048 and tubulin complex, the pharmacophore-based virtual screening was further employed to identify new anti-mitotic agents from a chemical database.

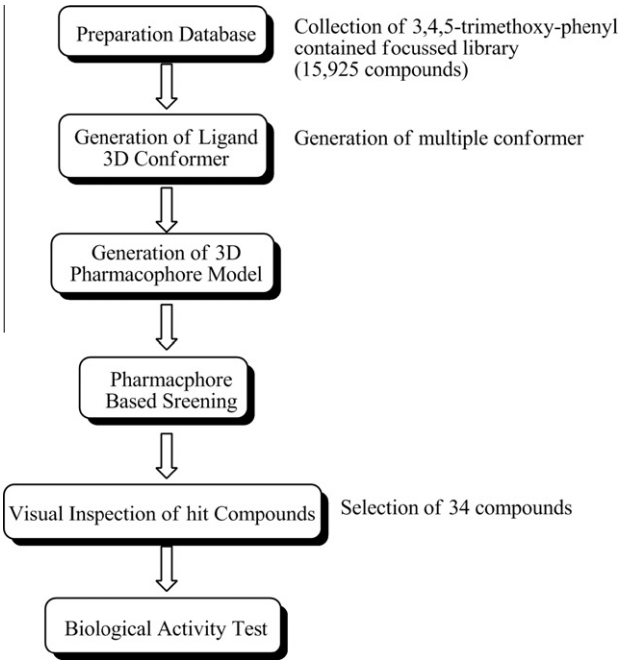

Figure 1. Summary of virtual screening used in this study. The process consists of preparation of the database and generation of a pharmacophore model, followed by virtual screening and prioritization with the compound selection step.

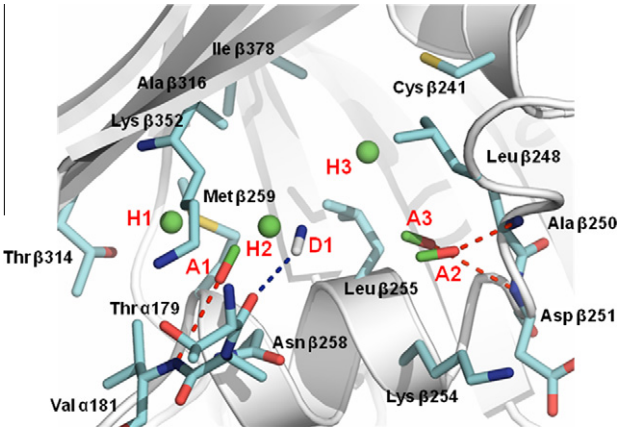

Figure 2. Pharmacophore generation of colchicine binding site of α/β-tubulin interface. The contact residues in the pharmacophore map are displayed with the colchicine binding site. A1, A2, A3, and D1 denote the three hydrogen bond acceptors and one hydrogen bond donor, respectively. H1, H2, and H3 represent hydrophobic interaction sites of ligand, respectively.

Table 1
Antiproliferative activities of virtually screened hit compounds

Compound	Structure	IC_{50}
1	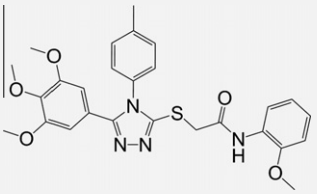	2.4
2	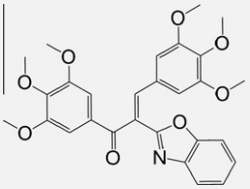	1.7
3	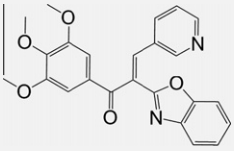	1.7
4	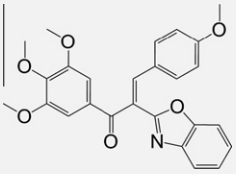	2.4
5	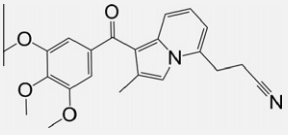	1.4
6	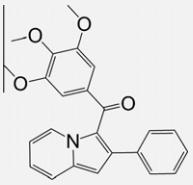	0.6
7	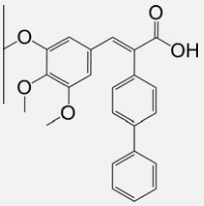	2.4
8	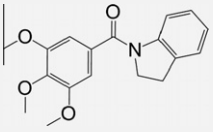	2.0
9	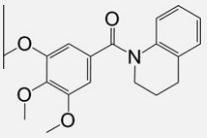	2.0
10	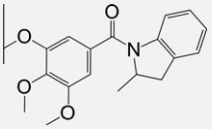	3.2

(*continued on next page*)

Table 1 (*continued*)

Compound	Structure	IC_{50}
11	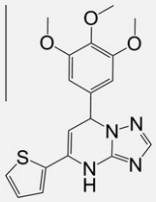	0.1
E7010[a]	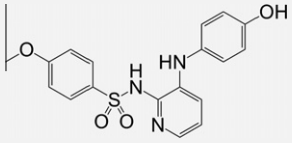	0.2

[a] **E7010** was used as a positive control.

Recently, Chiang et al. reported the identification of tubulin inhibitors targeting the colchicine binding site using ligand-based pharmacophore and virtual screening.[21] The Hypo 1 pharmacophore model, which was built on the basis of 21 training-set indole derivatives with varying levels of anti-proliferative activity, was utilized to screen the chemical database in silico and four compounds were identified. The most potent compound showed anti-proliferative activity with an IC_{50} of 187 nM. Alternatively, Nguyen et al.[22] used the X-ray structure of the complex to design a pharmacophore model for a diverse set of colchicine site ligands, ranging from colchicine itself to curacin A. Correlations between pharmacophoric elements of the ligands were obtained in 3D by aligning each ligand against colchicine and podophyllotoxin, followed by refinement using the molecular volume and electrostatic surface obtained from the X-ray structure data. The pharmacophoric points were derived from recurring tubulin-ligand interactions, and the overall pharmacophore for the colchicine-binding site consisted of a total of seven points. Each ligand possessed five or six elements of the overall pharmacophore.

In this study, we used the crystal structure of tubulin-colchicine complexes to perform pharmacophore-based virtual screening. The information obtained from the above-mentioned studies was considered before conducting this study. Biological evaluations of

Table 2
Tubulin polymerization inhibition data of compounds **5**, **6**, and **11**

Compound	**5**	**6**	**11**	**E7010**[a]
IC_{50} (μM)	5.0	20	12.8	8.0

[a] **E7010** was used as a positive control.

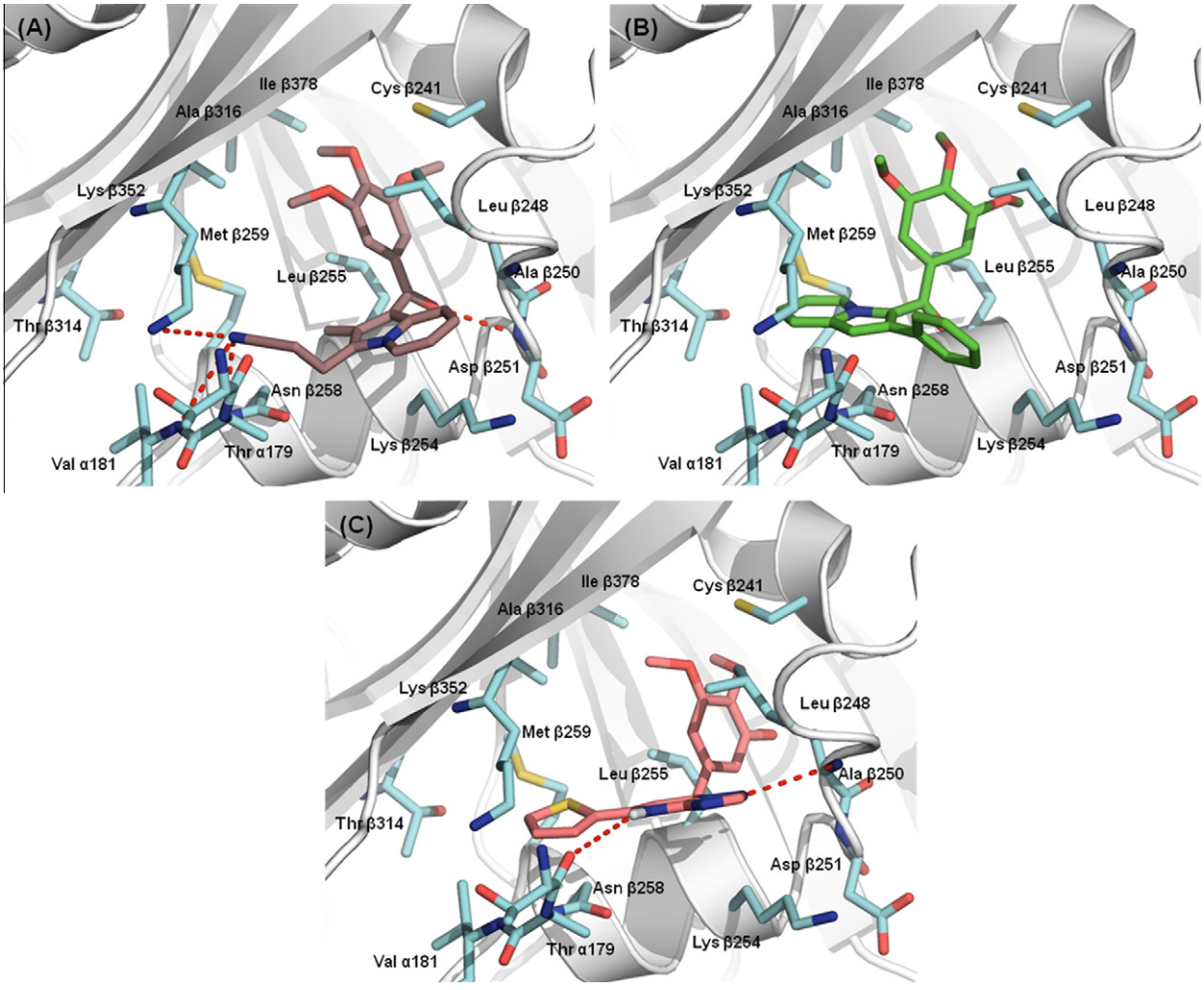

Figure 3. The refined docking model of compounds **5**, **6**, and **11** to tubulin. (A–C) Proposed binding mode of compounds **5**, **6**, and **11** to tubulin. The protein structure originated from the X-ray study of its complex with DAMA-colchicine (encoded as 1SA0 in PDB). Tubulin is shown in a ribbon representation and the residues of α/β-tubulin involved in the hydrogen bond interactions with compounds **6** and **11** are shown as dotted lines.

cell proliferation, in vitro inhibition of tubulin polymerization, and cell cycle arrest at the G_2/M phase revealed that compounds **5**, **6**, and **11** showed potent anti-mitotic and anti-proliferative activity and could serve as new lead compounds for the development of anti-cancer therapeutics.

2. Results and discussion

2.1. Virtual screening

Several X-ray crystal structures of complexes between β-tubulin and inhibitors of the colchicine binding site have been reported.[11–13] A large number of synthetic and natural compounds with diverse structures have been shown to bind at the colchicine site. For the virtual screening of tentative inhibitors targeting the colchicine binding site, we initially investigated the X-ray crystal structure of the β-tubulin complex with colchicine and podophyllotoxin.[12,23] Using these data, we built a pharmacophore map of all the interactions with amino acid residues that constitute the pocket on tubulin. For the generation of pharmacophore, we used the PharmoMap® program (Equispharm, Korea), a software package that enabled us to build a feature-based pharmacophore in which the pharmacophore points are represented by chemical features such as hydrogen bond acceptors/donors or hydrophobicity. The program built all the possible interactions that a ligand could establish with a given binding site. The overall process of virtual screening is presented in Figure 1.

2.2. Construction of focused library

Colchicine, podophyllotoxin and combretastatin A4 commonly contained the trimethoxyphenyl (TMP) group. In order to promote a more successful pharmacophore screening, we constructed a focused chemical library of compounds containing the TMP group. We searched for commercially available compounds harboring the TMP moieties within the in-house database. A total number of 15,925 commercially available chemical compounds were collected from the in-house chemical database. To find new active colchicine-binding site inhibitors, we prepared 3D pharmacophore queries for the structure-based virtual screening. As shown in Figure 2, the constructed pharmacophore consisted of three hydrogen bond acceptors (labeled as A1, A2, and A3), one hydrogen bond donor (D1), and three hydrophobic centers (H1, H2, and H3). We carried out virtual screening of the TMP focused library for the colchicine binding pocket using PharmoScan™ (Equispharm, Korea). Among the pharmacophore-based virtual screening hit compounds, those exhibiting unfavorable interactions with the binding site or adopting unrealistic conformations were

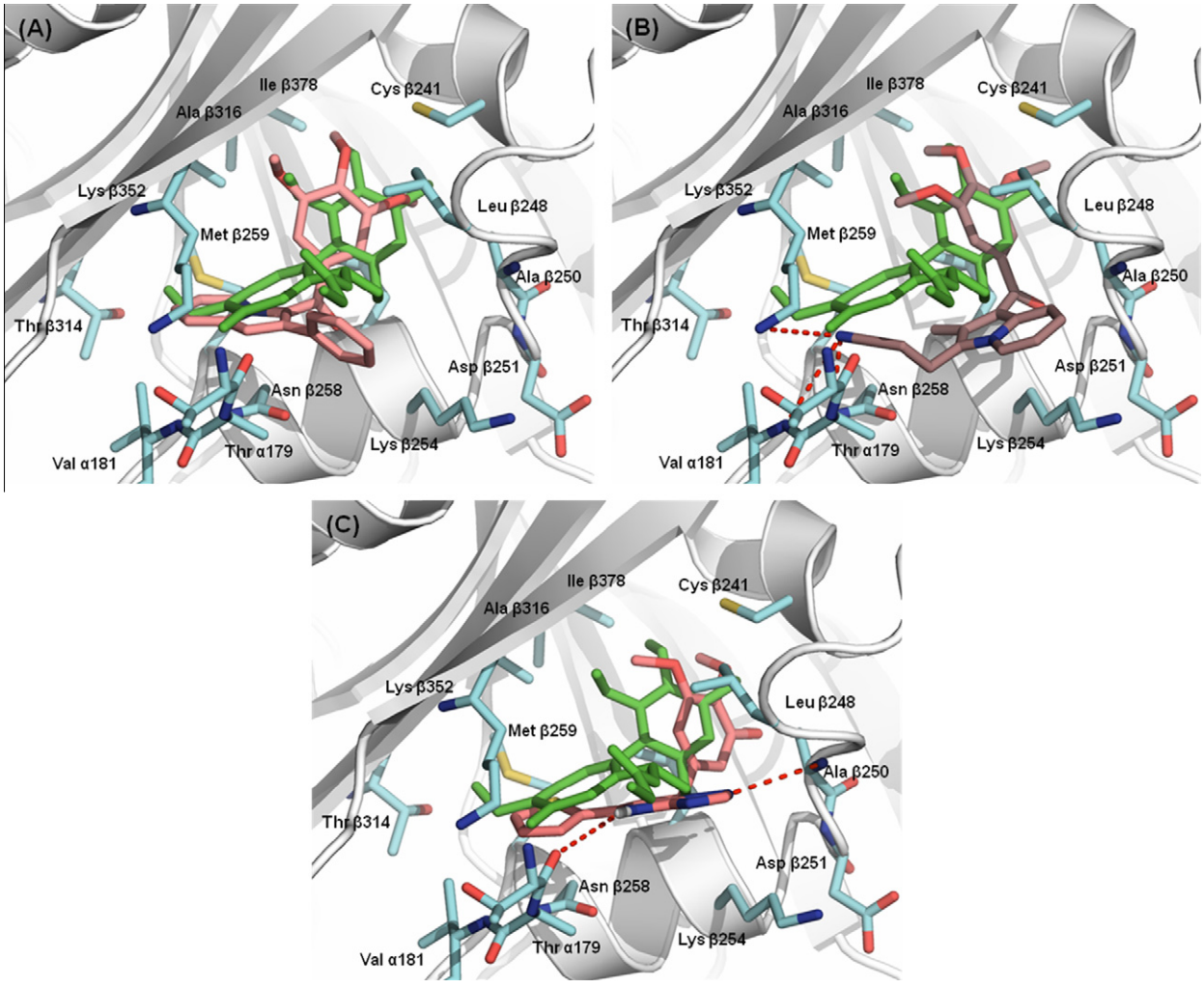

Figure 4. Comparison of the proposed binding modes of compounds **5**, **6**, and **11** to tubulin with that of DAMA-colchicine. Comparison of the DAMA-colchicine binding mode with those of compounds **5** (A), **6** (B), and **11** (C). DAMA-colchicine is presented in green. The refined docking model of compounds **5**, **6**, and **11** into α/β interface of tubulin was performed using the AUTODOCK4 program.

filtered out by visual inspection. Finally, we selected 34 compounds for further testing in vitro.

2.3. Biological evaluation of virtual screening hit compounds

In order to determine the activity of 34 virtually screened compounds, we evaluated the in vitro cell growth inhibition in the HL60 (Human promyelocytic leukemia) cell line using the MTT assay. The IC_{50} values represent the compound concentrations at which there was a 50% decrease in cell growth after 3 days of compound incubation. Eleven compounds had IC_{50} values of 0.1–3.2 μM in the MTT assay and each value is listed in Table 1. Compound **E7010**, which binds the colchicine site of tubulin, was used as a positive control

We further tested whether the eleven compounds directly interacted with tubulin and inhibited tubulin polymerization in vitro. As shown in Table 2, among the eleven compounds, compounds **5**, 6, and **11** inhibited tubulin polymerization with IC_{50} values of 20, 12.8, and 5 μM, respectively. These values were comparable to the activity of **E7010**. However, the other eight compounds showed low activity in the in vitro tubulin polymerization assay.

2.4. Molecular docking analysis of tubulin polymerization inhibitors

It should be noted that compounds **5**, **6**, and **11** showed not only cell growth inhibition, but also inhibited tubulin polymerization in vitro. These results demonstrate that the newly identified compounds **5**, **6**, and **11** can directly interact with the colchicine binding pocket on tubulin. To further elucidate the interactions between compounds **5**, 6, and **11** and tubulin, a molecular docking study was performed. First, we investigated the binding modes of compounds **5**, 6, and **11** to the colchicine binding pocket on tubulin. The results of the molecular docking study are summarized in Figure 3. The docking study revealed that the 3,4,5-TMP group of each compound was bound to the colchicine-binding site via hydrophobic interaction with Leu 248, Ala 250, Leu 255, and Ala 316 of tubulin, respectively.

The indolizine moiety of compound **5** served as a π–π interaction site with the non-aromatic residue of the side chain of Asn 258 in β-tubulin. In addition, the phenyl ring of compound **5** was located at the α/β interface of tubulin (Fig. 3a). In the case of compound **6**, the nitrile group interacted with Val 181, Lys 352 side chain and Asn 258 side chain in β-tubulin. The carbonyl group in compound **6** served as a hydrogen bond acceptor to the amino group of the main chain of Asp 251 (Fig. 3b). The docking model of compound **11** suggests the hydrogen bond interaction between the compound and Thr 179 in the backbone of α-tubulin and Ala 250 in the main chain of β-tubulin (Fig. 3c). By analyzing the results of the docking studies, we found that the 3,4,5-TMP group of compounds **5**, 6, and **11** was structurally overlapped with the 3,4,5-TMP rings of both podophyllotoxin and colchicine in the tubulin complex (Fig. 4).

2.5. Biological activities test of virtual screen hit analogues and their functional analysis

As shown in Tables 1 and 2, compound **11** exhibited strong antiproliferative activity with inhibition of tubulin polymerization in vitro. In order to validate the activity of the chemical scaffold of the virtually screened hit compounds and to further identify compounds showing better activity, we searched for commercially available derivatives of compounds **5**, 6, and **11**. While we could not find any derivatives of compounds **5** and **6**, the derivatives of compound **11** were obtained from commercial sources. As shown in Table 3, we then tested the compound **11** derivatives for cell anti-proliferative activity in the HL-60 cell line and the inhibition of tubulin polymerization in vitro. We finally obtained three

Table 3
Anti-proliferative activities and tubulin polymerization inhibition of compound **11** derivatives

Compound	Structure	IC_{50} (μM)	
		HL60	ITP[a]
12	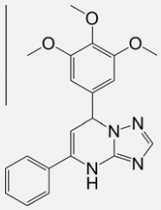	0.17	13.7
13	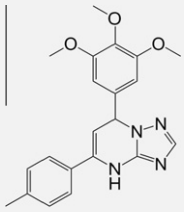	0.13	12.8
14	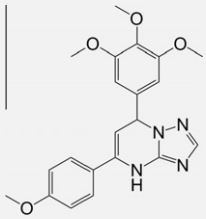	0.19	10.4
15	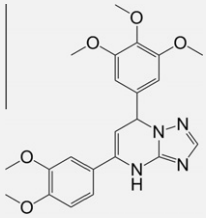	0.34	>24
16	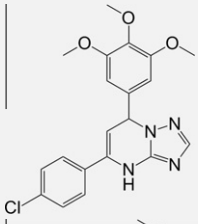	0.39	>25
17	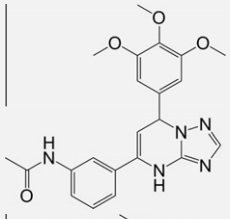	0.33	>25
18	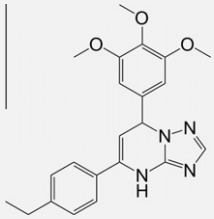	0.37	>25
E7010	—	0.2	8.0

[a] ITP: Inhibition of tubulin polymerization; **E7010** was used as a positive control.

compound **11** derivatives, compounds **12**, 13, and **14**, which showed strong activity in HL-60 cell growth inhibition.

To validate and compare the cell cytotoxic activity of the identified compounds, HL60 cells were treated with various concentrations of each compound for 48 h. The cytotoxic effects induced by treatment with the compounds (**11**–**14**) were analyzed by flow cytometry as described in Section 4. Each compound caused apoptotic cell death in a concentration-dependant manner (Fig. 5). EC_{50} values for each compound were calculated using flow cytometry data. The EC_{50} values of compounds **12**–14 revealed about 2–6-fold more activity than **E7010** (Table 4). Among these, compound **13** exhibited the most potent cytotoxic activity against HL-60 cells (EC_{50} = 0.07 μM).

To determine whether the apoptotic cell death induced by treatment with the compounds was caused by cell cycle arrest at G2/M phase, in which the tubulin polymerization reaction is essential, we performed cell cycle analysis using flow cytometry. HL60 cells were treated with a single concentration (0.1 μM or 0.5 μM, depending on their EC_{50} values) of each compound for 24 h. Flow cytometric analysis at an early time point (24 h) showed that compound **13** strongly arrested the cells at G2/M phase (Fig. 6). However, the other compounds did not induce cell cycle arrest at G2/M phase at least until 24 h incubation. At 48 h incubation, all compounds induced apoptosis as shown in Figure 5. To analyze the binding mode of compound **13** with tubulin, we performed a molecular docking study of compound **13** and compared it with those of colchicine and podophyllotoxin (Fig. 7). Comparison of the X-ray structure-derived binding mode of colchicine and podophyllotoxin with the docking model of compound **13** (Fig. 7B and C) showed that they share very similar binding shapes, confirming the cell data of compound **13** as shown in Table 4. In detail, the

Table 4
Apoptosis induction by compound **11** derivatives[a)]

Compound	**11**	**12**	**13**	**14**	**E7010**
Activity (EC_{50}, μM)	0.78	0.22	0.07	0.08	0.45

[a] Determination of EC_{50} values for each compound was calculated based on the Figure 5 data of cell cycle analysis. Note that the concentrations for compounds **12**–**14** are much lower than those of other compounds.

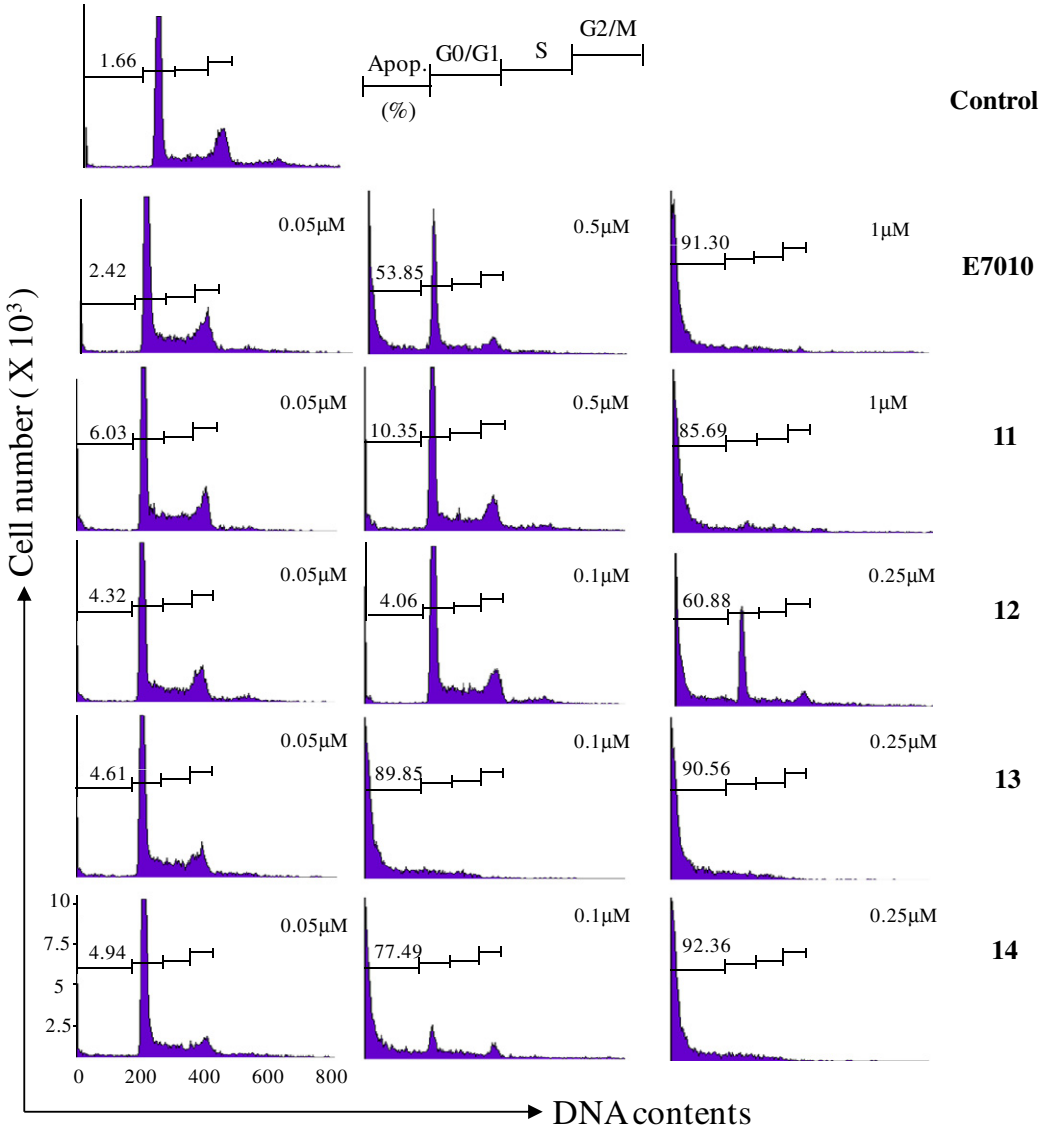

Figure 5. Cytotoxicity and EC_{50} analysis by flow cytometry. Flow cytometric analysis of cytotoxicity using HL-60 cells treated with different concentrations of the indicated compounds. Cells were treated with compounds for 48 h and the apoptotic fractions were determined using flow cytometry. The percentages of apoptotic cells (Apop in legend) were indicated. Data are representative of at least three independent experiments.

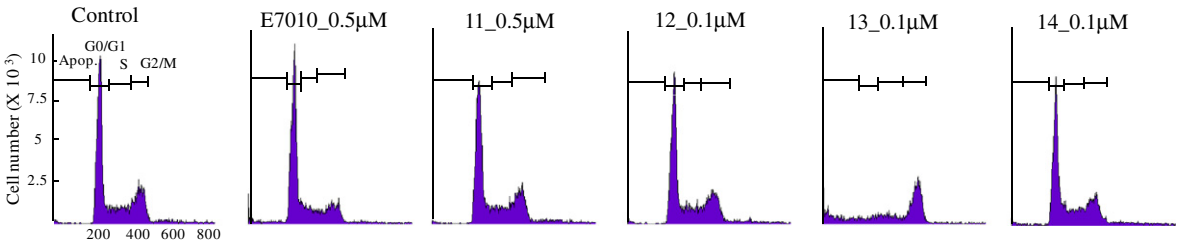

	Control	E7010	11	12	13	14
Apop.	0.53%	3.45%	0.48%	0.81%	22.94%	0.93%
GO/G1	55.47%	58.6%	53.87%	53.51%	9.70%	51.67%
S	17.62%	15.14%	15.16%	15.92%	16.50%	18.82%
G2/M	22.26%	19.96%	25.93%	25.82%	48.64%	24.39%

Figure 6. Cell cycle arrest at G2/M phase by treatment of compounds. HL60 cells were treated with each compound at the indicated concentrations for 24 h followed by cell cycle analysis using flow cytometry. Percentage of each cell cycle was calculated and shown in Table 4. Note that strong cell cycle arrest at G2/M phase was observed by treatment with compound **13**.

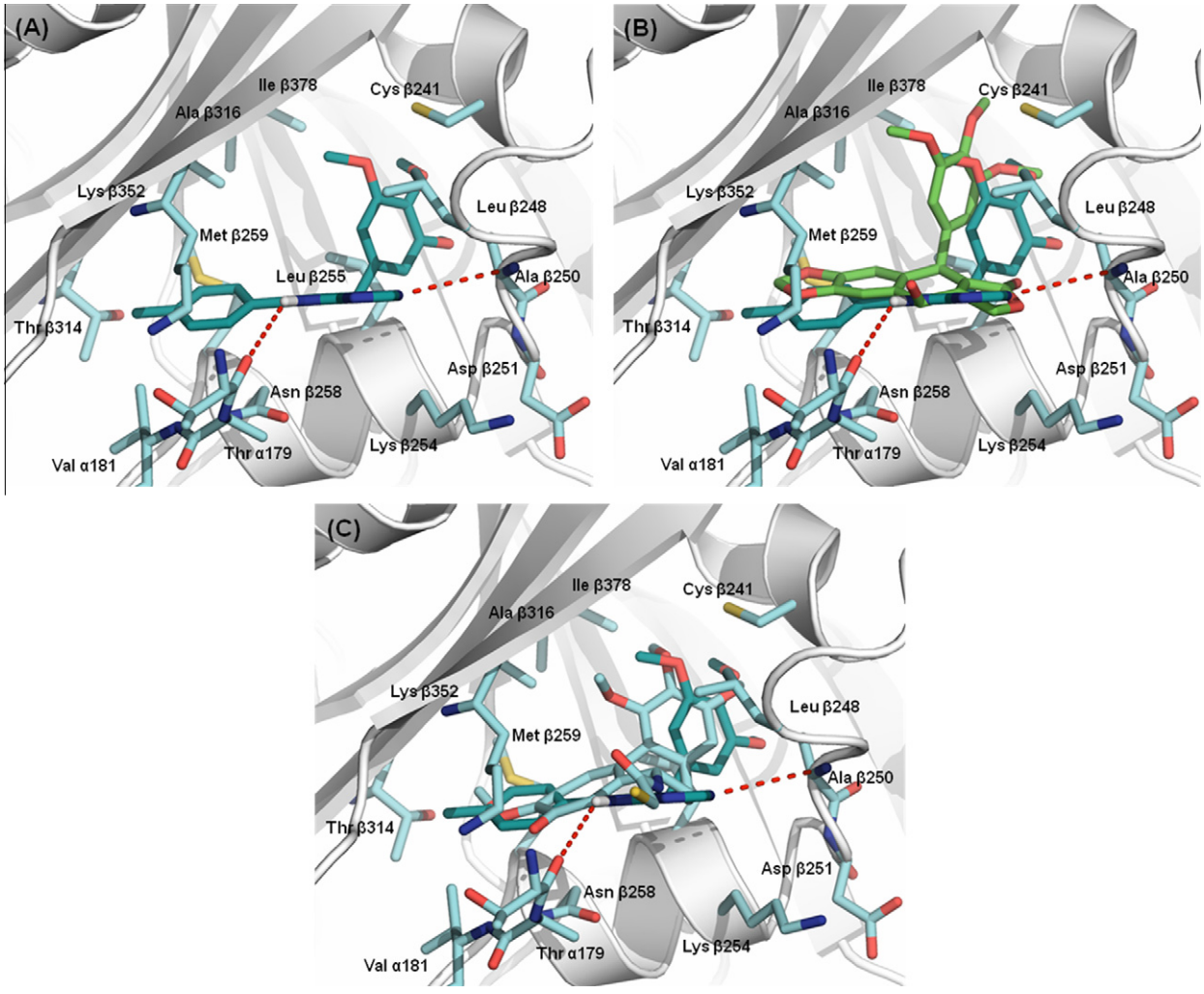

Figure 7. The molecular docking model of compound **13** with tubulin. (A) Proposed binding mode of compound **13** to tubulin. The red dotted lines indicate the potential hydrogen bonding between Thr α179, Ala β250 and compound **13**. (B and C) Comparison X-ray structure-based binding modes of podophyllotoxin (green color) and DAMA-colchicine (cyan color) with the docked conformation of compound **13**.

4-methyl-phenyl ring of compound **13** interacted with Val 181, Lys 352 side chain and Asn 258 side chain in β-tubulin. The binding mode of compound **13** proposes the hydrogen bond interaction between the compound and Thr 179 in the backbone of α-tubulin and Ala 250 in the main chain of β-tubulin, respectively (Fig. 7A). These data demonstrate that compound **11** derivatives can be used as strong anti-mitotic agents.

3. Conclusions

In this study, we present a successful application of pharmacophore-based virtual screening to identify novel compounds with strong anti-mitotic activity based on their ability to inhibit tubulin polymerization. The hit compounds selected by pharmacophore-based virtual screening were initially assayed in HL60 cell growth inhibition and tubulin polymerization assays. Among the hit compounds, compounds **5**, 6, and **11** showed strong anti-proliferative activity against HL60 cancer cell lines and also effectively inhibited tubulin polymerization in vitro. We further validated the binding model by virtually screening the hits and testing the cytotoxic activity, cell cycle arrest, and the inhibition of tubulin polymerization in vitro. Among these, the derivatives of compound **11** consistently exhibited potent activities and merit further evaluation as novel anti-mitotic agents. Furthermore, the proposed pharmacophore and docking model of compounds **5**, **6**, and **11** would provide useful information for the development of new chemical entities of microtubule-targeted anti-cancer agents.

4. Materials and methods

4.1. Molecular docking study

To refine the docking models of compounds **5**, **6**, and **11** into the colchicine binding site of tubulin, automated docking simulation was performed with AUTODOCK4.[24] The X-ray crystal structure of tubulin from Protein Data Bank (PDB code 1SA0)[12] was used for our docking simulation. For the docking, the structure of tubulin was kept rigid whereas all the torsional bonds in compounds **5**, 6, and **11** were set free to perform flexible docking. The binding energy between protein and inhibitors was evaluated using atom affinity potentials that were pre-calculated on grid maps using AutoGrid. The grid maps had dimensions of $40 \times 40 \times 40$ Å with 0.375 Å spacing between grid points. In AUTODOCK4, docking was performed by combining a global genetic algorithm with local minimization, Lamarckian genetic algorithm. One hundred trials were performed for each docking, and the final docked conformations were clustered using a tolerance of 1 Å root-mean-square deviation (RMSD). The docking conformation properly oriented toward the colchicine binding pocket was selected, and the free energy of binding was estimated. The molecular graphics of the possible colchicine binding pocket and the refined docking model with compounds **5**, 6, and **11** were generated using PyMol package (http://www.pymol.org).

4.2. Virtual screening

To search for possible colchicine binding site inhibitors, the pharmacophore was analyzed using PharmoMap™, Equispharm's in-house software package for structure-based virtual screening.[18] Constructed pharmacophore models were feature-based, that is, the pharmacophoric points are presented by chemical features, such as hydrogen bond acceptors/donors and hydrophobic features. The pharmacophore models were employed as search queries to identify colchicine binding site inhibitors from a 3D small molecule database, which is a focused library of commercially available multi-conformers containing the 3,4,5-trimethoxyphenyl (TMP) group. Structure-based virtual screening for possible inhibitors at the colchicine binding pocket on tubulin was carried out using the PharmoScan™ (Equispharm, Korea) as described.[18,25,26] Among the hit compounds found in the virtual screening, compounds exhibiting unfavorable interactions between the ligand and the binding site or adopting unrealistic conformations were filtered out by visual inspection.

4.3. Cell culture

Human promyelocytic leukemia (HL-60) cell lines were maintained in RPMI 1640 supplemented with penicillin/streptomycin (1%) and heat-inactivated FBS (10%). Cells were grown at 37 °C in a 5% CO_2 humidified incubator.

4.4. Cell proliferation assay

Cells (2×10^4 cells) were seeded into 96-well plates. After 24 h, the cells were grown in the presence or absence of compounds for another 48 h. After removing the 100 μl supernatant from each well, 20 μl of CellTiter 96 Aqueous solution (Promega, USA) were added into each well containing 100 μl of culture medium, and the cells were further incubated for 2 h at 37 °C in a humidified atmosphere of 5% CO_2. The reduction of absorbance at 490 nm was measured. IC_{50} values for each compound were determined by calculating the concentrations of 50% inhibition of cell proliferation.

4.5. Tubulin polymerization assays

HTS-Tubulin Polymerization Assay Kit (Cat. No. BK004/CDS01, Cytoskeleton, USA) was used for in vitro tubulin polymerization assay as described by previous report.[18] All components were added to micro-wells kept at 0 °C, and baselines were established at 340 nm. Assembly was followed sequentially at 0 and 37 °C, and tubulin assembly was measured turbidometrically using Molecular Device SPECTRA MAX Plus model (Molecular Devices, USA) equipped with electronic temperature controllers.

4.6. Apoptosis and cell cycle analysis

The effects of compounds on cell cycle and apoptosis were analyzed using flow cytometry as described by Kim do et al.[26] Briefly, human promyelocytic leukemia HL60 cells (3×10^5) were seeded in 6-well plates. After 24 h incubation, the cells were further grown in the presence of carrier (DMSO) alone or test compounds for 24 h and 48 h. Cells were harvested by centrifugation, washed with PBS and fixed in chilled 70% ethanol at −20 °C. The cells were then centrifuged to remove the fixative, washed and suspended in PBS containing 100 μg/ml of RNase A and 50 μg/ml of propidium iodide, and kept in the dark for 30 min to stain DNA. The cell cycle was analyzed by flow cytometry (Becton Dickinson FACScalibur). A total of 10,000 cells were counted for each determination. Apoptotic cells were determined by measuring the fractions of fragmented DNA. All flow cytometry analyses were performed in at least three independent experiments.

Acknowledgements

This work was supported in part by National Research Foundation of Korea Grant funded by the Korean Government (KRF-2008-314-C00269), a grant from the Korea Healthcare Technology R&D Project, Ministry for Health, Welfare & Family Affairs, Republic of Korea (A084826).

References and notes

1. Erickson, H. P.; O'Brien, E. T. *Ann. Rev. Biophys. Biomol. Struct.* **1992**, *21*, 145.
2. Purich, D. L.; Kristofferson, D. *Adv. Protein Chem.* **1984**, *36*, 133.
3. Desai, A.; Mitchison, T. J. *Annu. Rev. Cell Dev. Biol.* **1997**, *13*, 83.
4. Hammond, J. W.; Cai, D.; Verhey, K. J. *Curr. Opin. Cell Biol.* **2008**, *20*, 71.
5. Nogales, E.; Wang, H. W. *Curr. Opin. Cell Biol.* **2006**, *18*, 179.
6. Downing, K. H. *Annu. Rev. Cell Dev. Biol.* **2000**, *16*, 89.
7. Honore, S.; Pasquier, E.; Braguer, D. *Cell. Mol. Life Sci.* **2005**, *62*, 3039.
8. Pellegrini, F.; Budman, D. R. *Cancer Invest.* **2005**, *23*, 264.
9. Jordan, M. A.; Wilson, L. *Nat. Rev. Cancer* **2004**, *4*, 253.
10. Long, B. H.; Carboni, J. M.; Wasserman, A. J.; Cornell, L. A.; Casazza, A. M.; Jensen, P. R.; Lindel, T.; Fenical, W.; Fairchild, C. R. *Cancer Res.* **1998**, *58*, 1111.
11. Gigant, B.; Wang, C.; Ravelli, R. B.; Roussi, F.; Steinmetz, M. O.; Curmi, P. A.; Sobel, A.; Knossow, M. *Nature* **2005**, *435*, 519.
12. Ravelli, R. B.; Gigant, B.; Curmi, P. A.; Jourdain, I.; Lachkar, S.; Sobel, A.; Knossow, M. *Nature* **2004**, *428*, 198.
13. Cormier, A.; Marchand, M.; Ravelli, R. B.; Knossow, M.; Gigant, B. *EMBO Rep.* **2008**, *9*, 1101.
14. Kavallaris, M. *Nat. Rev. Cancer* **2010**, *10*, 194.
15. Yin, S.; Bhattacharya, R.; Cabral, F. *Mol. Cancer Ther.* **2010**, *9*, 327.
16. Henriquez, F. L.; Ingram, P. R.; Muench, S. P.; Rice, D. W.; Roberts, C. W. *Antimicrob. Agents Chemother.* **2008**, *52*, 1133.
17. McGrogan, B. T.; Gilmartin, B.; Carney, D. N.; McCann, A. *Biochim. Biophys. Acta* **2008**, *1785*, 96.
18. Kim, D. Y.; Kim, K. H.; Kim, N. D.; Lee, K. Y.; Han, C. K.; Yoon, J. H.; Moon, S. K.; Lee, S. S.; Seong, B. L. *J. Med. Chem.* **2006**, *49*, 5664.
19. Weisenberg, R. C.; Borisy, G. G.; Taylor, E. W. *Biochemistry* **1968**, *7*, 4466.
20. Edwards, M. L.; Stemerick, D. M.; Sunkara, P. S. *J. Med Chem.* **1990**, *33*, 1948.
21. Chiang, Y. K.; Kuo, C. C.; Wu, Y. S.; Chen, C. T.; Coumar, M. S.; Wu, J. S.; Hsieh, H. P.; Chang, C. Y.; Jseng, H. Y.; Wu, M. H.; Leou, J. S.; Song, J. S.; Chang, J. Y.; Lyu, P. C.; Chao, Y. S.; Wu, S. Y. *J. Med. Chem.* **2009**, *52*, 4221.
22. Nguyen, T. L.; McGrath, C.; Hermone, A. R.; Burnett, J. C.; Zaharevitz, D. W.; Day, B. W.; Wipf, P.; Hamel, E.; Gussio, R. *J. Med. Chem.* **2005**, *48*, 6107.
23. Dorléans, A.; Gigant, B.; Ravelli, R. B.; Mailliet, P.; Mikol, V.; Knossow, M. *Proc. Natl. Acad. Sci. U.S.A.* **2009**, *106*, 13775.
24. Morris, G. M.; Huey, R.; Lindstrom, W.; Sanner, M. F.; Belew, R. K.; Goodsell, D. S.; Olson, A. J. *J. Comput. Chem.* **2009**, *30*, 2785.
25. Ryu, K.; Kim, N. D.; Choi, S. I.; Han, C. K.; Yoon, J. H.; No, K. T.; Kim, K. H.; Seong, B. L. *Bioorg. Med. Chem.* **2009**, *17*, 2975.
26. Kim, N. D.; Yoon, J.; Kim, J. H.; Lee, J. T.; Chon, Y. S.; Hwang, M. K.; Ha, I.; Song, W. J. *Bioorg. Med. Chem. Lett.* **2006**, *15*, 3772.
27. Kim, K. H.; Kim, N. D.; Seong, B. L. *Expert Opin. Drug Discovery* **2010**, *5*, 205.